ORIGINAL PAPER

COMPENSATION OF THERMAL EFFECT ON NONINVASIVE BLOOD GLUCOSE MONITORING IN OPTICAL COHERENCE TOMOGRAPHY

SAID AMRANE[1], NAWFEL AZAMI[1], MOSTAFA ABOURICHA[2]

Manuscript received: 15.08.2016; Accepted paper: 08.10.2016;
Published online: 30.12.2016.

Abstract. *Noninvasive glucose monitoring techniques based on optical coherence tomography (OCT) are affected by several per-turbing factors which must be taken into account, for example, variation of tissue temperature. Herein a direct method to detect the change in skin temperature based on the comparison of the peak levels that characterize the OCT signal during noninvasive OCT-based glucose monitoring is presented. A process is described for real time calibration and compensation of the induced error on blood glucose due to thermal effect by numerical analysis of B-scan OCT images.*

Keywords: *Compensation; glucose monitoring; noninvasive; OCT; thermal effect.*

1. INTRODUCTION

Monitoring of blood glucose, noninvasively and contin-uously, is a current need. There are several approaches for developing a noninvasive blood glucose meter including optical coherence tomography (OCT) [1]. OCT is a high-resolution imaging technique and can be applied to noninvasive glucose monitoring [2-4]. However, noninva-sive glucose monitoring techniques based on OCT are af-fected by several perturbing factors, including variation of tissue temperature, which can be controlled by a temperature control module integrated in an optical scanning probe to take account of this factor [5].

In this study, the possibility of direct detection of the variation of skin temperature based on the comparison of the peak levels that characterize the OCT signal during OCT-based noninvasive glucose monitoring is demonstrated.

A process is described for real time calibration and com-pensation of thermal induced error on blood glucose moni-toring using B-scan OCT.

2. OCT IMAGING

Optical coherence tomography is a noninvasive imaging technique with high resolution in depth. It uses the Michelson interferometer illuminated by a low coherence light for imaging biological tissue to an imaging depth of a few millimeters. The depth resolution can be in the micron range [6]. An OCT system, based on optical fibers [7], is shown in Fig. 1.

[1] National Institute of Telecommunications INPT, Optics department, 10000, Rabat, Morocco.
[2] Faculty of science Ain Chock, Hassan II University, LERSD, Casablanca, Morocco.
E-mail: saidph1974@gmail.com; azami@inpt.ac.ma; mmabouricha@gmail.com.

The coupler (or beam splitter) splits the broad-band-source light into two parts. One part is sent to the ref-erence arm while the other is sent to the sample arm. After the roundtrip, interference of the light from the two arms allows axial information to be extracted for each position of the reference mirror. Translating the reference mirror allows a sample reflectance profile to be obtained in the axial direction, the so-called "A-scan". The "B-scan" shows a transverse cut (two-dimensional [2D] image).

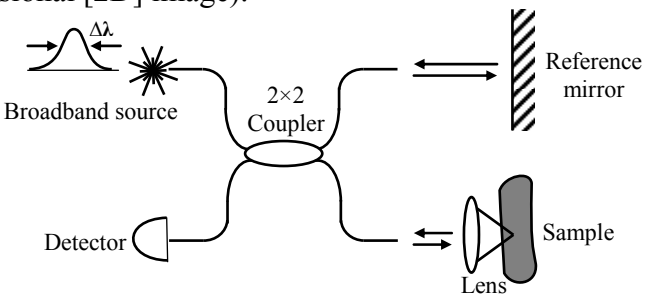

Figure 1. OCT system principle.

The "C-scan" allows the construction of a three-dimensional image [8, 9]. Interferences are detected only if $\delta \leq lc$, where lc is the coherence length of the illumination source and δ is the optical path difference between the two arms. The axial resolution is then equal to the source coherence length lc. In the case of a Gaussian spectrum source, the coherence length is given by the following equation [10]:

$$l_c = \frac{2\ln 2\lambda_0^{\,2}}{\pi\Delta\lambda} \tag{1}$$

where Δλ is the spectral width of the broadband light source and λ_0 its central wavelength.

The transverse resolution of OCT imaging is the same as that of conventional optical microscopy. It is given by the following mathematical formula [6]:

$$\Delta x = \frac{4\lambda_0 f}{\pi d} \tag{2}$$

where d is the spot size on the objective lens and f is its focal length.A two dimension B-scan OCT image is illustrated in Fig. 2.

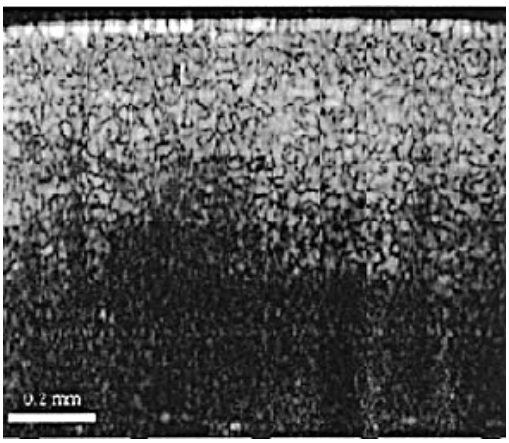

Figure 2. Typical B-scan skin OCT image.

Major skin layers are easily distinguishable. The black region on the upper side of the image is the air region for which backscattering is negligible. The epidermis is the white

region near the surface. Papillary dermis is also visible since scattering in this region is more important than the junction region. The light intensity in the image is then de-creasing that represents the reticular dermis region. We will discuss on the next section the importance on the reticular dermis region to measure the blood glucose.

3. OCT AND GLUCOSE MEASUREMENT

The coefficient of attenuation (μt) of a ballistic photon, in a medium with a scattering coefficient (μ_s) and absorption coefficient (μ_a), can be expressed as $\mu_t=\mu_a+\mu_s$. Since absorption in biological tissues is substantially less than scattering ($\mu_a<<\mu_s$) in the near-infrared spectral range [11], the Beer–Lambert law can be expressed as follows:

$$I = I_0 e^{-\mu_s z} \tag{3}$$

I_0 is the incident light intensity, and I is the light intensity at depth z. Therefore, the exponential attenuation of ballistic photons in tissue is mainly dependent on the scattering co-efficient μs. Since μs of the tissue changes with glucose con-centration, the exponential profile of light attenuation in tissue is dependent on the glucose concentration [11]. Therefore, one can monitor the glucose concentration by measuring the exponential slope of light attenuation in tis-sue with the OCT technique [4, 12].

The 2D OCT image is averaged in the lateral direction (z-axial) into a one-dimensional (1D) curve to obtain an OCT signal that represents 1D distribution of light in depth [11] to suppress the speckle noise and minimize motion artifacts and thereby improve the measurement precision of optical tissue properties [13].

OCT signals are plotted in a logarithmic scale and the slope of the signals is calculated at specific depths by the linear least-squares method. To obtain the best correlation be-tween the current blood glucose concentration and the slope of the OCT signal, the OCT signal slope is calculated at different depths. The signal slope is used to calculate blood glucose concentration [4, 12]. Fig. 2 shows a typical 2D image of the skin, and Figure 3 shows a typical dis-tribution of the signal in one dimension with two maximum peaks which are caused by the two bright reflecting bands. The epidermis lies between the surface and the local inten-sity minimum. The second peak is caused by the reflection of dermal fibers. The layer between the first minimum and the second maximum peak corresponds to the junction of epidermis and the upper dermis, known as the papillary layer. Thus, the border of the dermis is characterized by the second maximum peak [14, 15].

4. APPROACH FOR COMPENSATION OF THERMAL EFFECT

4.1. DIRECT READING OF TEMPERATURE VARIATION ON OCT SIGNAL

This paragraph shows theoretically that the variation of temperature can be directly derived from the measurement of the coordinates of the two characteristic peaks of OCT signal previously described.

Fig. 3 shows the typical shape of a skin OCT signal taken from a forearm of a human.

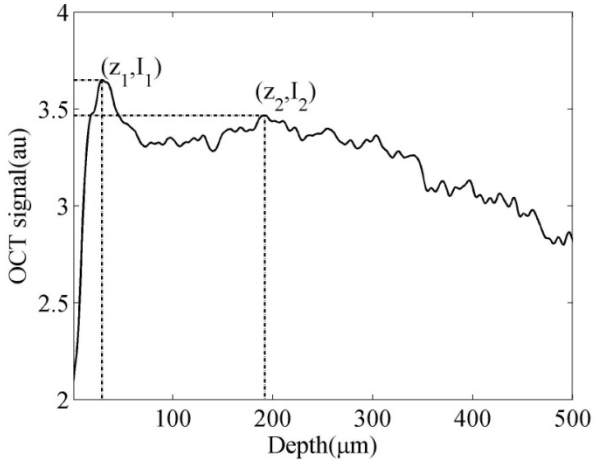

Figure 3. Typical one-dimensional OCT signal obtained from aver-aging A-scan OCT signal.

where (Z_1, I_1) and (Z_2, I_2) are the coordinates of the two peaks that characterize the signal. The first peak (Z_1, I_1) is due to the reflection of the surface skin. The second peak (Z_2, I_2) is caused by the reflection of dermal fibers. The border of the dermis is characterized by the second maxi-mum peak (Z_2, I_2) as has been described in ref [14, 15].

The intensity of the two peaks depends on the skin temper-ature T due to the dependence of μt of the temperature, which is of the order of $\partial\mu t/\partial T=0.006$ mm^{-1}/°C [5, 16].

$$\mu_t(T+\Delta T)=\mu_t(T)+\frac{\delta\mu_t}{\delta T}\Delta T \tag{4}$$

$$I_i(T)=R_iI_0\exp[-\mu(T)z_i] \quad i=1, 2\ldots \tag{5}$$

where R_i (i=1, 2) is the coefficient of reflection in depth z_i.

If r and r' are the ratios between the intensities of the two peaks at the temperature T and T'=T+ΔT respectively, one can write:

$$r=\frac{R_1}{R_2}\exp[-\mu(T)(z_1-z_2)] \tag{6}$$

$$r'=\frac{R_1}{R_2}\exp[-\mu(T')(z_1-z_2)] \tag{7}$$

$$r'=r\exp\left[-\frac{\delta\mu}{\delta T}\Delta T(z_1-z_2)\right] \tag{8}$$

$$r'\approx r\left[1-\frac{\delta\mu}{\delta T}\Delta T(z_1-z_2)\right] \tag{9}$$

Let us define the percent variation of the ratio between the intensities of the two peaks due to thermal effect as Δr/r. One can write:

$$\frac{\Delta r}{r}=\frac{r'-r}{r}\approx\frac{\delta\mu}{\delta T}\Delta T\Delta z \tag{10}$$

$$\Delta T\approx\left(\frac{\Delta r}{r}\right)\left(\frac{\delta\mu}{\delta T}\Delta z\right) \tag{11}$$

Eqn. (11) is obtained by the Taylor expansion to the first order. $\Delta r/r$ is proportional to $\delta\mu/\delta T$, Δz and ΔT. With knowledge of the ratio of $\Delta r/r$, one can derive the variation of the temperature ΔT. Eqn. (11) clearly shows that the temperature variation can be detected by measuring the ratio between the two mainly peaks as well as the variation of this ratio $\Delta r/r$ and the depth Δz between these peaks. Since temperature variation can be derived, one can numerically compensate the contribution of temperature on the blood glucose by direct OCT measurement. The OCT scan is then theoretically sufficient to measure both slope and temperature variation without the need of an external temperature controller module. Next section describes the simulations that are performed to be able to compensate thermal effect on blood glucose measurement.

4.2. PROCESS FOR REAL TIME ERROR COMPENSATION ON BLOOD GLUCOSE CONCENTRATION

Previous section theoretically describes the impact of temperature fluctuation on the percent variation intensity OCT peaks $\Delta r/r$. Hence, at this step, we have shown that temperature variation can be directly derived from a numerical peak analysis on the OCT signal.

Our goal is to automatically compensate thermal effect on the OCT signal slope and by the way on the blood glucose. In the following, a process is proposed for real time compensation. Let us consider a patient for which we have to monitor the blood glucose using OCT.

At the beginning, an experimental B-scan OCT image have to be performed in ambient temperature conditions T_0 (Fig. 2). By averaging this B-scan data one can derive 1D-OCT signal intensity as a function of the depth (figure 3). Numerical analysis can be performed to derive the parameters needed in eqn. (11) which are $\Delta r/r$ and the slope p as well as the depth Δz between the two peaks. Note that the slope p is used to calculate blood glucose concentration as described in ref [4, 12].

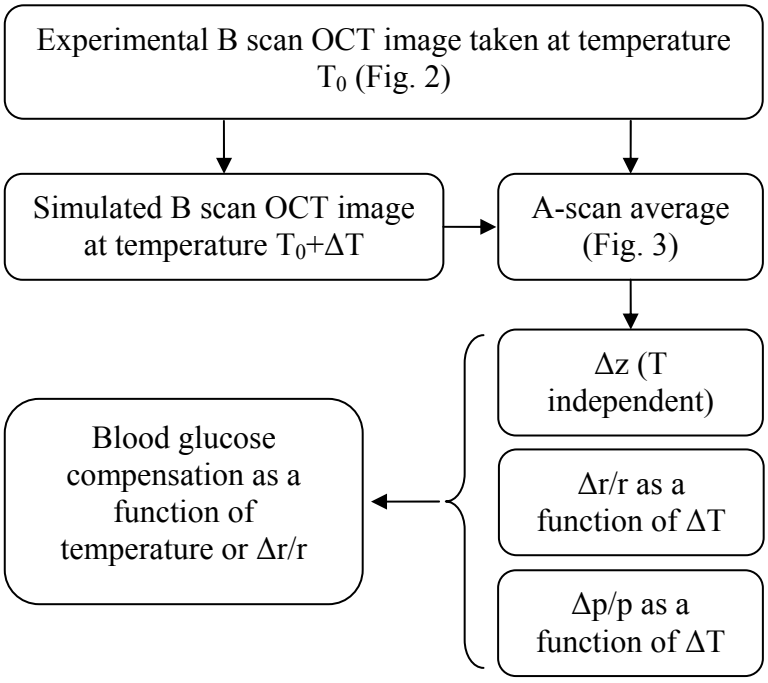

Figure 4. Procedure to record parameters for calibration and compensation of blood glucose.

Simulations are then performed to derive B-scan images at different temperature from the initial B-scan image referenced at temperature T_0. Note that these simulated images are derived from an initial B-scan image which correspond to a given blood glucose. Hence all simulated images have a blood glucose that remains the same. To do this, pixels intensities are re-calculated by introducing thermal effect on the attenuation coefficient as is mentioned in eqn. (4). For the same blood glucose and at a temperature $T_0+\Delta T$, the OCT signal slope can be calculated taking into account the variation of the scattering coefficient μs caused by ΔT as described by the temperature dependence referenced in [5, 16]. These simulations allow us to have enough data with a high resolution on the correspondence between percent variation $\Delta r/r$, percent variation of slope $\Delta p/p$ and ΔT. These data are stored to be able to monitor and compensate any variation due to thermal effect for this particular patient.

Numerical processing on OCT B-scan images are performed using Matlab to derive the OCT signal slope for different temperature conditions. The OCT signal slope, designated as p, can be calculated by linear regression for an image taken at a temperature T. The procedure is briefly described in the following Fig. 4. The final result is a correspondence between the percent variation $\Delta r/r$ (Eqn. 10) and the percent variation of the OCT signal slope $\Delta p/p$.

4.3. RESULTS AND DISCUSSIONS

The simulated curves that represent the variation of OCT signal and its slope as a function of the depth for different values of temperature are illustrated in Fig. 5.

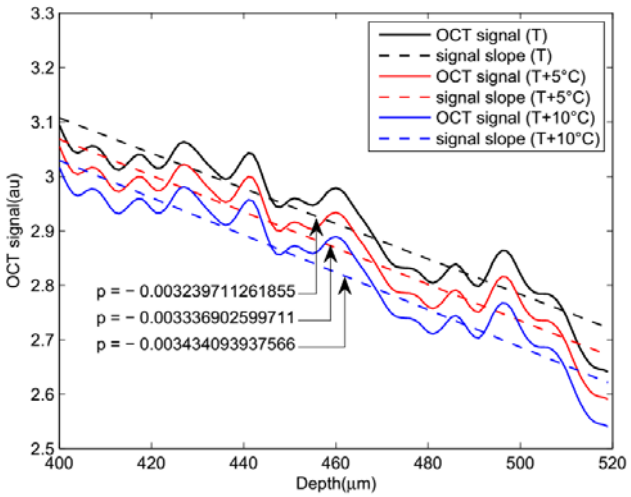

Figure 5. Zoom of part of the OCT signal and slope at different temperatures.

The solid curves in Fig. 5 represent the OCT detected signal at the dermis junction for different temperatures. The dashed curves are the OCT signal slope obtained by using the linear regression method. It appears that the p slope is changing as a function of temperature for a given blood glucose concentration. From these simulated images, a numerical analysis is performed to derive percent variations $\Delta r/r$ and $\Delta p/p$ due to thermal deviation of the scattering coefficient (Fig. 6a).

Thermal effects must be compensated on the p slope before using it for the calculation of the blood glucose con-centration. Numerical investigations, as described in last section, allow us to make a correspondence between per-cent variation of OCT peaks intensities ratio and percent variation of the slope due to thermal effect affecting both parameters. From the

procedure described in Fig. 4, sim-ulated compensation on the slope as a function of Δr/r ratio is plotted in Fig. 6b.

Our proposition is to generate automatically this calibra-tion curve for a patient to compensate thermal effect on the final blood glucose concentration reading. Taking into account the results presented in [12] where the variation of 10 mg/dl of glucose has been presented to cause an aver-age variation of 1.9% of the OCT signal slope, one can de-rive the compensation curve of blood glucose as a function of percent variation OCT peak intensities Δr/r (Fig. 6c).

For example, a temperature variation of 5°C corresponds to a variation Δr/r of 0.46% by using Δz=160 μm (numeri-cally measured on averaged OCT signal for a given patient) and$\delta\mu/\delta T$ =0.006 mm^{-1}/°C [13]. Using calibration curve presented in Fig. 6c, this percent variation of Δr/r due to 5°C thermal variation induce an error on the measured blood glucose that should be corrected with 14.7 mg/dl.

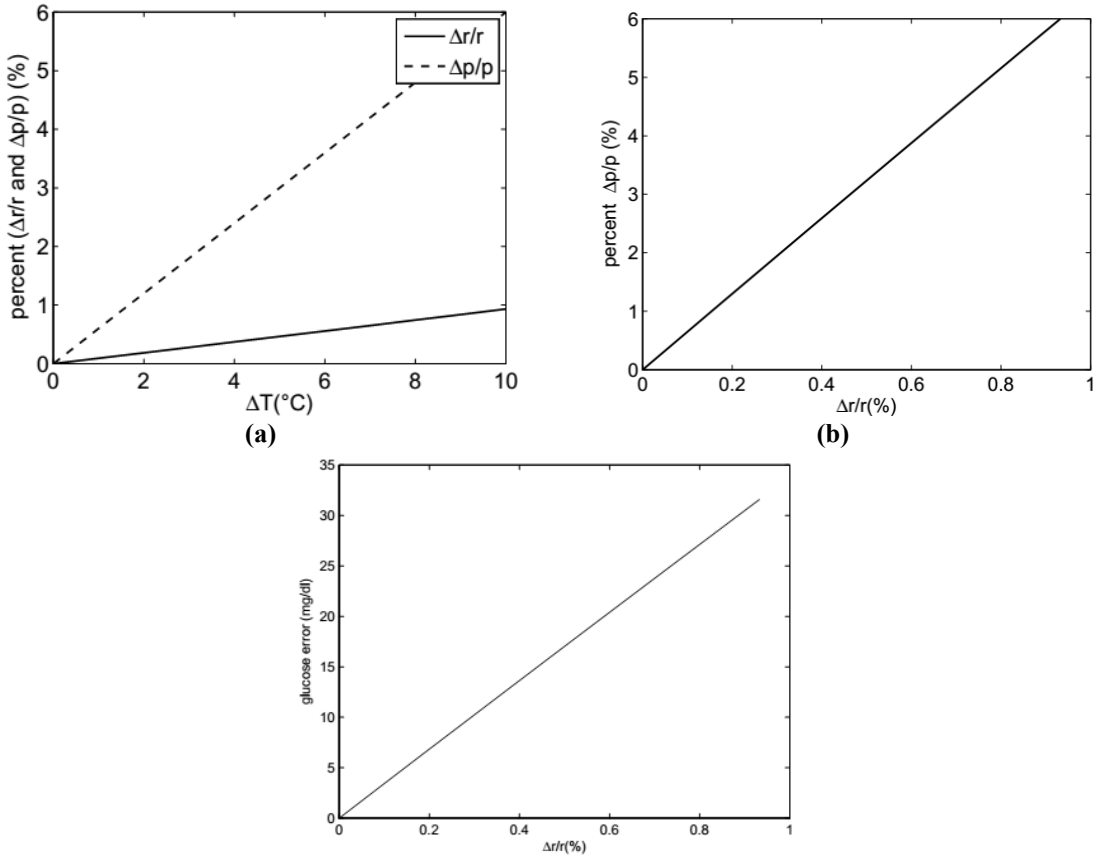

Figure 6. (a) Simulated Percent variation of OCT signal peak intensities Δr/r and slope Δp/p as a function of temperature variation. (b) Simulated percent variation Δp/p as a function of percent variation Δr/r. (c) Simulated blood glucose concentration error (mg/dl) as a function of OCT peak intensities percent variation Δr/r.

4. CONCLUSION

We propose a method based on OCT to detect the change in the skin temperature simultaneously with blood glucose monitoring in order to offset the effect of this drift by correcting the OCT signal slope that is correlated with blood glucose levels. We will carry out experimental study to validate this result at a future date.

REFERENCES

[1] So, C.F., Choi, K.S., Wong, T.K., Chung, J.W., *Med Devices (Auckl)*, **5**, 45, 2012.
[2] Sapozhnikova, V.V., Prough, D., Kuranov, R.V., Cicenaite, I., Esenaliev, R.O., *Exp Biol Med (Maywood)*, **231**(8), 1323, 2006.
[3] Ghosn, M.G., Sudheendran, N., Wendt, M., Glasser, A., Tuchin, V.V., Larin, K.V., *J Biophotonics*, **3**(1-2), 25, 2010.
[4] Esenaliev, R.O., Larin, K.V., Larina, I.V., Motamedi, M., *Opt Lett*, **26(**13), 992, 2001.
[5] Su, Y., Meng, Z., Wang, L.Z., Yu, H.M., Liu, T., *Chin Opt Lett*, **12**(11), 111701, 2014.
[6] Drexler, W., Fujimoto, J.G., *Optical coherence tomography: technology and applications*. Springer, Berlin, 2015.
[7] Huang, D., Swanson, E.A., Lin, C.P., Schuman, J.S., Stinson, W.G., Chang, W., Hee, M.R., Flotte, T., Gregory, K., Puliafito, C.A., Fujimoto, J.G., *Science*, **254**(5035), 1178, 1991.
[8] Fujimoto, J.G., Brezinski, M.E., Tearney, G.J., Boppart, S.A., Bouma, B., Hee, M.R., Southern, J.F., Swanson, E.A., *Nat Med*, **1**(9), 970, 1995.
[9] Tearney, G.J., Bouma, B.E., Boppart, S.A., Golubovic, B., Swanson, E.A., Fujimoto, J.G., *Opt Lett*, **21**(17), 1408, 1996.
[10] Brezinski, M.E., *Optical coherence tomography: principles and applications*, Academic Press, 2006.
[11] Larin, K.V., Motamedi, M., Ashitkov, T.V., Esenaliev, R.O., *Phys Med Biol*, **48**(10), 1371, 2003.
[12] Larin, K.V., Eledrisi, M.S., Motamedi, M., Esenaliev, R.O., *Diabetes Care*, **25**(12), 2263, 2002.
[13] Kuranov, R.V., Sapozhnikova, V.V., Prough, D.S., Cicenaite, I., Esenaliev, R.O., *Phys Med Biol*, **51**(16), 3885, 2006.
[14] Hori, Y., Yasuno, Y., Sakai, S., Matsumoto, M., Sugawara, T., Madjarova, V., Yamanari, M., Makita, S., Yasui, T., Araki, T., Itoh, M., Yatagai, T., *Opt Express*, **14**(5), 1862, 2006.
[15] Welzel, J., *Skin Res Technol*, **7**(1), 1, 2001.
[16] Khalil, O.S., Yeh, S.J., Lowery, M.G., Wu, X., Hanna, C.F., Kantor, S., Jeng, T.W., Kanger, J.S., Bolt, R.A., de Mul, F.F., *J Biomed Opt*, **8**(2), 191, 2003.